Received: 22 April 2025 | Revised: 18 July 2025 | Accepted: 23 July 2025

DOI: 10.1002/dad2.70165

Alzheimer's & Dementia
Diagnosis, Assessment & Disease Monitoring

RESEARCH ARTICLE

Accounting for white matter uptake improves between tracer agreement in amyloid PET

Yinghua Chen[1,2] | Hillary Protas[1,2] | Ji Luo[1,2] | Shan Li[1,2] | Javad Sohankar[1,2] | Chen-Ray Pan[3] | Valentina Ghisays[1,2] | Wendy Lee[1,2] | Teresa Wu[4,5] | Ding-Geng Chen[6,7] | Eric M Reiman[1,2,8,9] | Kewei Chen[1,2,6,10] | Yi Su[1,2,4,5,10]

[1]Banner Alzheimer's Institute, Phoenix, Arizona, USA

[2]Arizona Alzheimer's Consortium, Phoenix, Arizona, USA

[3]Basis Chandler, Chandler, Arizona, USA

[4]ASU-Mayo Center for Innovative Imaging, Tempe, Arizona, USA

[5]School of Computing and Augmented Intelligence, Tempe, Arizona, USA

[6]College of Health Solutions, Arizona State University, Phoenix, Arizona, USA

[7]Department of Statistics, University of Pretoria, PRETORIA, South Africa

[8]Biodesign Institute, Arizona State University, Tempe, Arizona, USA

[9]Department of Psychiatry, University of Arizona, Tucson, Arizona, USA

[10]Department of Neurology College of Medicine-Phoenix, Phoenix, Arizona, USA

Correspondence
Yi Su, Banner Alzheimer's Institute, 901 E Willetta Street, Phoenix, AZ 85006, USA.
Email: yi.su@bannerhealth.com

Abstract

INTRODUCTION: Amyloid positron emission tomography (PET) allows in vivo measurement of amyloid plaque deposition; however, different tracers lead to different results. We test the hypothesis that the variability in amyloid measurements is related to white matter retention, and accounting for this variability can improve agreements.

METHODS: Data from the Centiloid project was downloaded and processed for four F18 tracer-to-Pittsburgh Compound B (PiB) pairs to obtain mean cortical standardized uptake value ratio (MCSUVR). Three approaches were examined to account for white matter contribution to the MCSUVR. Pearson's correlation was used to assess the between tracer agreements. Steiger's test was used to determine the significance of improvement.

RESULTS: Accounting for white matter signal improves the agreement. The regional spread function partial volume correction (RSF PVC) method was most consistent in achieving statistically significant improvements ($p < 0.05$) for all four tracer pairs.

DISCUSSION: Between-tracer agreement of amyloid measure can be improved by accounting for white matter signal. Further investigation is ongoing for additional improvement.

KEYWORDS
amyloid, harmonization, PET

Highlights

- Analyzing head-to-head data for all four common F18-labeled tracers against Pittsburgh Compound B (PiB).
- Evaluating three different techniques to correct for white matter signal.
- Steiger's test to determine the significance of improvements.
- White matter uptake contributes to the between-tracer measurement difference.

1 | INTRODUCTION

Amyloid is a hallmark pathology of Alzheimer's disease (AD).[1] Amyloid plaques are detectable at least 15 years before the onset of AD symptoms,[2] and the prevalence of amyloid positivity increases as a function of age, even in cognitively normal individuals.[3] Several radiolabeled imaging tracers have been developed and validated to detect and quantitatively measure amyloid burdens in vivo using positron emission tomography (PET) techniques.[4–8] These tracers are widely used in AD research, including many clinical trials that use amyloid PET imaging to assess treatment efficacy and target engagement as surrogate biomarkers.[9–12] A large multicenter study, Imaging Dementia-Evidence for Amyloid Scanning (IDEAS), has also been conducted to determine the clinical usefulness of amyloid PET and paved the way for clinical adoption of this technology.[13] Amyloid PET has begun to play an important role in clinical care with the development of successful anti-amyloid treatments.[14,15]

Currently, there are five widely used amyloid PET tracers: the C11-labeled Pittsburgh Compound B (PiB),[4] and four F18-labeled tracers, florbetapir (FBP),[5] florbetaben (FBB),[6] flutemetamol (FTE),[7] and NAV4694 (NAV).[8] Although all of these PET tracers were designed to target brain amyloid pathology, each tracer has its unique characteristics of target binding affinity, kinetic behavior, and nonspecific retention; therefore, the imaging data acquired and the associated measurements are tracer dependent. This inter-tracer variation can be observed both visually and via quantitative measures.[16–19] The recently proposed Centiloid approach[20] defined a common numerical scale and partially addressed the variability in PET-derived amyloid measures across different tracers. However, the measurements still have the same level of correlation between tracers, and the inherent signal-to-noise property also remains the same after the conversion to the Centiloid scale.[21,22]

We hypothesize that the variability observed between tracers in measuring amyloid burden is partly due to partial volume effects arising from the inherently low spatial resolution of PET imaging and signal spillover from white matter. While amyloid PET tracers are designed to selectively bind to amyloid plaques, emerging research indicates that some may also bind to myelin, which is abundant in white matter.[23–26] The combined effects of the tracer-dependent white matter signals, inter-individual variability in white matter tracer binding, and the partial volume effects can lead to the increased between-tracer differences in amyloid measurements. In this research, we test the hypothesis that accounting for the white matter signal can improve between-tracer agreement and reduce noise in the amyloid burden PET measures. To validate this hypothesis, we test three different strategies to decontaminate amyloid PET measures from white matter signal and evaluate their impact in improving between-tracer agreement and reducing measurement noise.

RESEARCH IN CONTEXT

1. **Systematic review**: We examined recent studies comparing amyloid positron emission tomography (PET) tracers and the Centiloid method, which standardizes amyloid PET measurements across tracers and analysis pipelines. We also reviewed research on using amyloid PET to assess white matter integrity, given structural similarities between amyloid plaques and myelin. While the Centiloid scale aids standardization, variability in signal-to-noise ratio and nonspecific uptake—particularly from white matter—remains a challenge.
2. **Interpretation**: Our finding supports the hypothesis that differences in nonspecific tracer uptake, especially in white matter, contribute to inconsistencies between tracers. Adjusting for white matter signal improves agreement across different amyloid tracers.
3. **Future directions**: Further work is needed to refine techniques that minimize white matter signal contamination in amyloid PET. Improved correction methods will enhance between-tracer consistency, support consensus-based interpretations, and facilitate multi-center studies using multiple tracers.

2 | MATERIALS AND METHODS

2.1 | Cohorts

Paired amyloid PET data of four F18-amyloid PET tracers with matched C11-PiB scans and T1-weighted MRI were downloaded from the Centiloid project (www.gaain.org/centiloid-project). These cohorts and datasets have been described previously.[17–19,27] As summarized in Table 1, there are 46 pairs of FBP,[17] 35 pairs of FBB,[18] 74 pairs of FTE,[27] and 55 pairs of NAV,[19] all against PiB. Each cohort has a subset of young control participants and another subset of older AD patients to help establish the anchor points of the Centiloid model, with remaining additional participants who had varied cognitive and biomarker statuses to capture the heterogeneity of amyloid pathology. In total, there are 57 young health controls (mean age 33), 47 elderly healthy controls (mean age 69), 46 mild cognitive impairment (MCI) patients (mean age 74), 49 AD (mean age 69), 5 frontotemporal dementia patients (mean age 70), 3 at-risk participants (mean age 80), and 3 possible AD patients (mean age 67). Detailed summary of participant characteristics is provided in Table 1, and please refer to the original papers[17–19,27] for additional cohort-specific information and technical details of data acquisition.

TABLE 1 Study cohorts demographic table.

Group	FBP ($n = 46$)		FBB ($n = 35$)		FTE ($n = 74$)		NAV ($n = 55$)		Total N	Average age of 4 groups
	No. of subjects	Age (years)	No. of subjects	Age (years)	No. of subjects	Age (years)	No. of subjects	Age (years)		
Young healthy controls	13	27 ± 4	10	33 ± 8	24	37 ± 5	10	33 ± 7	57	33
Elderly healthy controls	6	66 ± 9	6	71 ± 8	10	57 ± 11	25	74 ± 8	47	69
At risk	3	80 ± 3								
MCI	7	80 ± 9	9	72 ± 5	20	73 ± 7	10	75 ± 9	46	74
Possible AD	3	67 ± 5								
AD	14	67 ± 8	8	69 ± 6	20	69 ± 10	7	73 ± 11	49	69
Frontotemporal dementia			2	74 ± 8			3	68 ± 5	5	70

Abbreviations: AD, Alzheimer's disease; FBB, florbetaben; FBP, florbetapir; FTE, flutemetamol; MCI, mild cognitive impairment; NAV, NAV4694.

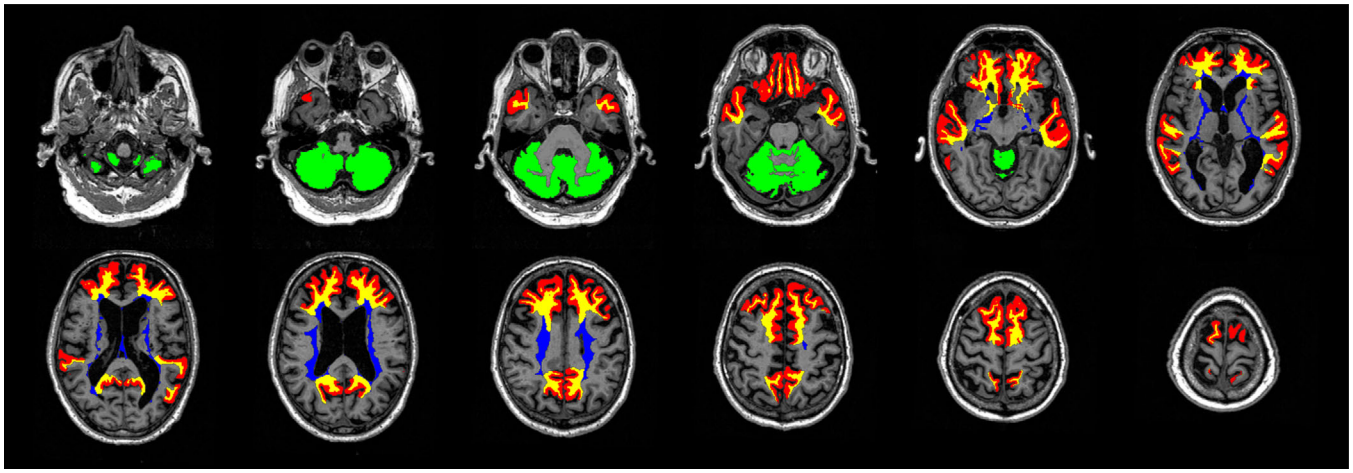

FIGURE 1 Illustration of ROIs for amyloid positron emission tomography (PET) quantification using the PET unified pipeline[29,30] as described in Section 2.2. The ROIs are color coded: cerebellum cortex (green), mean cortical region (red), white matter immediately adjacent to mean cortical region (yellow), and FreeSurfer defined UnsegmentedWhiteMatter (blue). PET, positron emission tomography; ROIs, regions of interest.

2.2 | Image analysis

FreeSurfer v7.3 (Martinos Center for Biomedical Imaging, Charlestown, Massachusetts, USA; https://surfer.nmr.mgh.harvard.edu/fswiki) was used to analyze T1-weighted MRI and define anatomical regions.[28] A PET unified pipeline (PUP; https://github.com/ysu001/PUP) was used to analyze PET data[29,30] and the procedure included resolution harmonization filtering,[31] inter-frame motion correction, PET-MR registration, target frame summation, regional intensity extraction, regional spread function (RSF) based partial volume correction (PVC),[29,32] and standard uptake value ratio (SUVR) calculation at regional and voxel level using the FreeSurfer defined left and right combined cerebellum cortex as the reference region. A mean cortical SUVR (MCSUVR)[30] was calculated as the target global amyloid burden measure. An illustration of relevant regions-of-interests is included in Figure 1.

Three approaches were used to reduce white matter signal spillover to the amyloid measure and test our hypothesis. In the first approach (white matter corrected [WMC]), the regional SUVR for the FreeSurfer defined UnsegmentedWhiteMatter (UWM) was used as a regressor to remove the white matter signal component from the MCSUVR and obtain the WMC version MCSUVR_WMC. In the second approach, a Richardson-Lucy (RL) iterative deconvolution technique,[33] implemented in MATLAB (The Mathworks, Inc., v2021a),[34] was used to deconvolve the SUVR images to improve image spatial resolution and reduce partial volume effects. In our experiment, the deconvolution was performed using the "deconvlucy" MATLAB function assuming an 8 mm full-width half-maximum (FWHM) Gaussian kernel as the point spread function and using 20 iterations and the default setting for other parameters. This size of the point spread function kernel is designed to match the spatial resolution of harmonized PET image generated from our analysis pipeline described above. Based on the deconvolved images, the MCSUVR_RL was then calculated for

TABLE 2 Strength of Pearson's correlation (*r*) between F18 tracer PET-derived MCSUVR and PiB MCSUVR_RSF with and without accounting for white matter signal.

	F18 Tracer	*N*	*r* (raw to PiB RSF)	*r* (corrected to PiB RSF)	Steiger's *P*
WMC	FBP	46	0.912	**0.959**	**0.000**
	FTE	74	0.951	**0.968**	**0.032**
	FBB	35	0.969	0.982	0.077
	NAV	55	0.975	0.973	0.760
RL	FBP	46	0.912	**0.923**	**0.013**
	FTE	74	0.951	0.952	0.819
	FBB	35	0.969	**0.974**	**0.005**
	NAV	55	0.975	**0.982**	**0.000**
RSF	FBP	46	0.912	**0.937**	**0.020**
	FTE	74	0.951	**0.974**	**0.000**
	FBB	35	0.969	**0.980**	**0.035**
	NAV	55	0.975	**0.987**	**0.000**
Centiloid	FBP	46	0.912	0.943	**0.001**
	FTE	74	0.951	0.959	**0.035**
	FBB	35	0.969	0.967	0.728
	NAV	55	0.975	0.972	0.281

Note: Values in bold indicate statistically improved agreements after correction.
Abbreviations: FBB, florbetaben; FBP, florbetapir; FTE, flutemetamol; MCSUVR, mean cortical standardized uptake value ratio; NAV, NAV4694; PiB, Pittsburgh Compound B; RL, Richardson-Lucy; RSF, regional spread function; WMC, white matter corrected.

performance evaluation. The third approach we evaluated here is the RSF-based PVC technique[29] implemented in PUP, which performs PVC on a regional basis and generates MCSUVR_RSF. The WMC method was implemented in R (version 4.3.2) using the "lm" function to derive the MCSUVR_WMC from the MCSUVR and UWM SUVR generated by PUP for both F18-based tracers and their matched PiB scans. MCSUVR_RL and MCSUVR_RSF were estimated for each tracer as described in the previous section. The Centiloid pipeline[20] derived MCSUVRs were also included for comparison.

2.3 | Statistical analysis

To evaluate the impact of white matter signal correction on agreement in global amyloid burden measurements, we used the Pearson's correlation coefficient as the benchmark measure, and the Steiger's test[35] was performed by using R package "bcdstats," function "test2r.steigerz1." This test compares the strength of two correlation coefficients that share a common reference variable, and in our case, the RSF-corrected PiB MCSUVR_RSF was used as the reference global amyloid burden measure. Using the WMC as an example, we tested whether the WMC-corrected F18 MCSUVR_WMC was more strongly correlated with PiB MCSUVR_RSF than the F18 MCSUVR without WMC. Significance was at the two-tailed 0.05 level to be conservative though our hypothesis is the inter-tracer SUVR harmonization improvement via the proposed corrections.

3 | RESULTS

The Pearson's correlation for raw F18-MCSUVR to PiB-MCSUVR_RSF ranged between 0.912 (FBP) and 0.975 (NAV) (Table 2). When using PiB-MCSUVR_RSF as the common reference to compare whether correcting for white matter signal improves between-tracer agreements, the Pearson's correlation improved numerically for almost all conditions except a small decrease for NAV with the WMC method (Table 2). The improvement was statistically significant ($p < 0.05$) for 9 out of the 12 total comparisons based on Steiger's test (Table 2). Scatter plots are also shown in Figure 2 to visually demonstrate the deviation of individual measurements from the regression line as well as the impact of methodological differences to the numerical values of MCSUVR. For comparison purposes, the Pearson's correlation and Steiger's test results were also reported for the Centiloid pipeline derived MCSUVR (Table 2). We observed better agreement between the Centiloid pipeline generated F18 tracer MCSUVR and the reference PIB measure for FBP and FTE, but not for FBB and NAV.

Overall, FBP had the lowest level of agreement with PiB measures, and NAV had the highest level of agreement. The RSF correction method had the most consistent impact on the between-tracer agreement and showed numerically and statistically significant improvements in all four comparisons. The impact of the WMC technique was the least consistent, leading to three numerical improvements with two of them statistically significant. It was also observed that the positive effects of correction methods to between-tracer agreement were

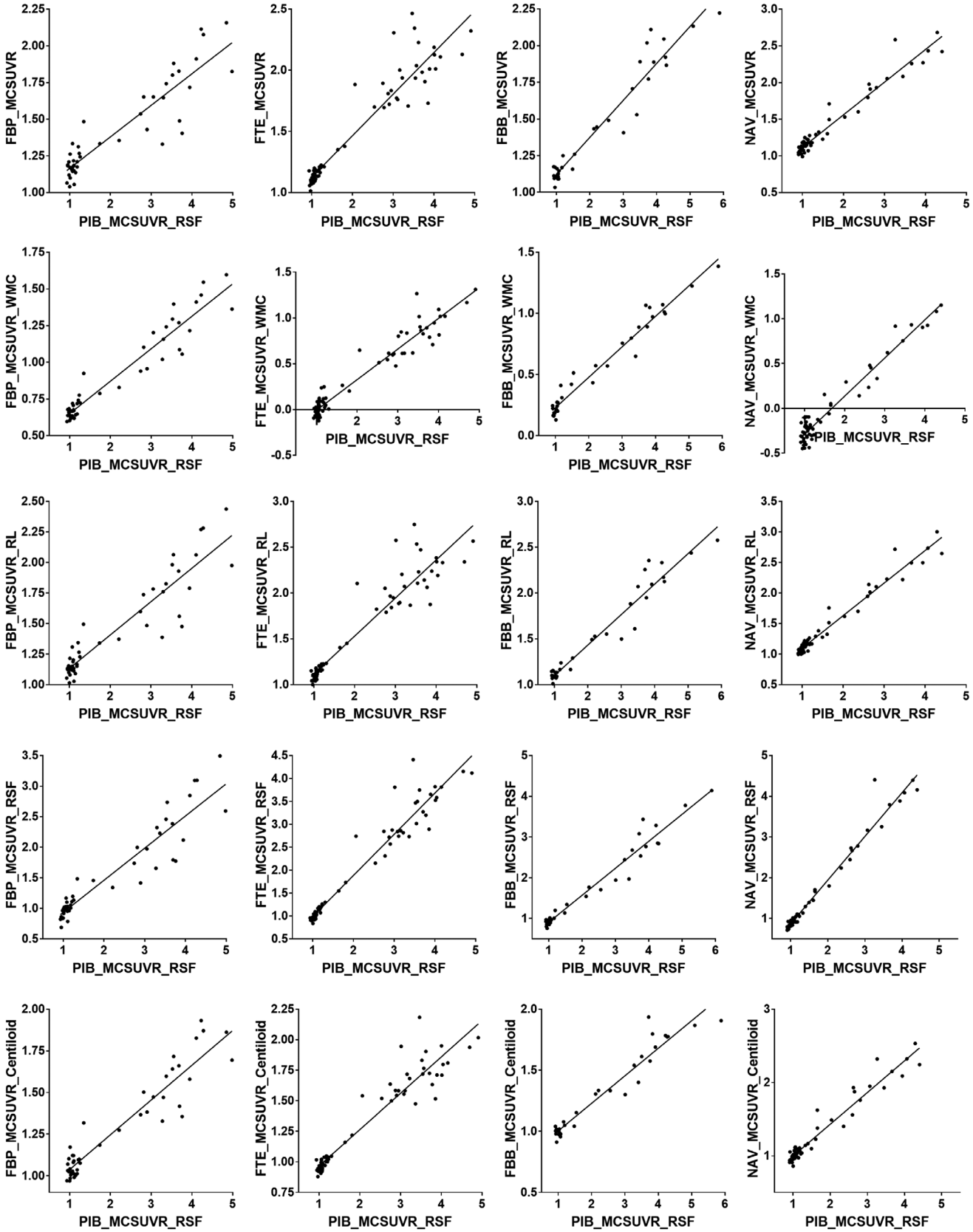

FIGURE 2 Scatter plots of F18 mean cortical SUVR measures against PiB derived MCSUVR with RSF correction. Each column is a different F18 tracer, from left to right, FBP, FTE, FBB, and NAV. Each row is a correction method, from top to bottom, no correction, WMC, RL, RSF, and Centiloid pipeline. FBP, florbetapir; FTE, flutemetamol; MCSUVR, mean cortical standardized uptake value ratio; NAV, NAV4694; PiB, Pittsburgh Compound B; RL, Richardson-Lucy; RSF, regional spread function; SUVR, standardized uptake value ratio; WMC, white matter corrected.

most consistent for FBP, which had the most inherent difference from PiB, where all three methods resulted in numerical and statistically significant improvements.

4 | DISCUSSION

In this research, we examined three techniques to account for white matter signal contamination to global amyloid burden measurements and evaluate their impacts on between-tracer measurement differences. It is found that correcting for white matter signal contamination generally leads to improved between-tracer agreements. The impact is more pronounced for tracers that behave more differently inherently. The RSF PVC technique led to the most consistent improvements across the four F18-based amyloid PET tracers. These results support the hypothesis that variabilities in white matter tracer uptake at least in part contribute to the tracer-dependent PET-derived amyloid measurements.

Among the three approaches we examined, the first approach, WMC, which takes into account for white matter uptake by using the measured white matter signal from the UWM region as the regressor to regress it out from the global amyloid burden measures, is less consistent and sometimes has detrimental effects. This may relate to the variation of white matter signals across the brain. The MCSUVR measure is derived from exclusively cortical regions and is relatively far away from the UWM, therefore, the UWM may not be an ideal region to be used as the regressor. In an exploratory analysis using the FreeSurfer-defined white matter regions immediately adjacent to the target region as the regressor, worse outcomes were observed. While the white matter signal component in the regressor is likely a better approximation of the contaminating white matter signal in the raw MCSUVR measure, the regressor also contains a substantial portion of true amyloid signal due to the spillover effects. Further optimization of this approach could be pursued in the future. The two other approaches are both designed for partial volume corrections. The RL technique achieves the goal by deconvolution and generating voxel-level corrections, while the RSF technique is designed for region-based corrections. For the intended goal of this research, the RSF technique performed slightly better, as demonstrated in our results section. Alternative strategies to quantify amyloid burden were also examined, for example, the Centiloid pipeline generated measures were in better agreement to PiB based measures for FBP and FTE while not for the other two tracers. When white matter was used as the reference region, the between tracer agreement was worse in our exploratory analysis. Further optimization of quantitative approaches to improve between-tracer agreements is warranted.

There are several limitations of this research. We focused on examining the agreement of global amyloid measures and did not examine the regional and voxel-level impact. We are currently investigating alternative techniques that can address this issue, and more research is needed to identify and develop techniques that can lead to the ultimate goal of interchangeable use of PET tracers designed for the same target. In order to investigate the effectiveness of correction methods, we used Steiger's test that required a shared variable to compare the strength of the correlations. While it is possible to choose other PiB measures as the reference, we choose RSF corrected PiB MCSUVR as we previously demonstrated the RSF correction improved signal to noise ratio and the sensitivity to detect amyloid positive scans and the statistical power to detect longitudinal changes.[16,36] The small to moderate cohort sizes in this study may also limit the generalization of the findings, however, the paired data is currently limited and the cost to acquire large datasets is prohibitive. Lastly, while the principle of techniques examined in this study could potentially be applied to other PET imaging targets such as tau PET, we did not examine that in this research.

In summary, this research demonstrated the effectiveness and potential utility of white matter signal correction techniques in improving amyloid PET measure harmonization across tracers. It supports the hypothesis that white matter tracer uptake variability contributes to the between tracer differences.

ACKNOWLEDGMENTS

The authors thank the study participants for their time and effort in participating in the various studies that contributed to the GAAIN Centiloid collection of head-to-head comparison amyloid PET data.

The research is supported by RF1AG073424, R01AG069453, P30AG072980, the Arizona Department of Health Services (ADHS), and the State of Arizona, ADHS Grant No. CTR057001. The funding sources did not play a role in study design, the collection, analysis, and interpretation of data, the writing of the report, or the decision to submit the article for publication.

All studies were approved by their corresponding institutional review boards, and written informed consent was obtained for each participant.

CONFLICT OF INTEREST STATEMENT

The authors have no conflicts of interest to report. Author disclosures are available in the Supporting Information.

ORCID

Yinghua Chen https://orcid.org/0000-0001-8810-0978

REFERENCES

1. Long J, Holtzman D. Alzheimer disease: an update on pathobiology and treatment strategies. *Cell*. 2019;179(2):312-339.
2. Bateman RJ, Xiong C, Benzinger TL, et al. Clinical and biomarker changes in dominantly inherited Alzheimer's disease. *N Engl J Med*. 2012;367(9):795-804.
3. Jansen WJ, Ossenkoppele R, Knol DL, et al. Prevalence of cerebral amyloid pathology in persons without dementia: a meta-analysis. *JAMA*. 2015;313(19):1924-1938.
4. Mathis CA, Wang Y, Holt DP, Huang G, Debnath ML, Klunk WE. Synthesis and evaluation of 11C-labeled 6-substituted 2-arylbenzothiazoles as amyloid imaging agents. *JMedChem*. 2003;46(13):2740-2754.
5. Wong DF, Rosenberg PB, Zhou Y, et al. In vivo imaging of amyloid deposition in Alzheimer disease using the radioligand 18F-AV-45 (florbetapir [corrected] F 18). *J Nucl Med*. 2010;51(6):913-920.

6. Barthel H, Gertz H, Dresel S, et al. Cerebral amyloid-beta PET with florbetaben (18F) in patients with Alzheimer's disease and healthy controls: a multicentre phase 2 diagnostic study. *Lancet Neurol*. 2011;10(5):424-435.
7. Nelissen N, Van Laere K, Thurfjell L, et al. Phase 1 study of the Pittsburgh compound B derivative 18F-flutemetamol in healthy volunteers and patients with probable Alzheimer disease. *J Nucl Med*. 2009;50(8):1251-1259.
8. Cselényi Z, Jönhagen ME, Forsberg A, et al. Clinical validation of 18F-AZD4694, an amyloid-beta-specific PET radioligand. *J Nucl Med*. 2012;53(3):415-424.
9. Rios-Romenets S, Lopera F, Sink KM, et al. Baseline demographic, clinical, and cognitive characteristics of the Alzheimer's Prevention Initiative (API) Autosomal-Dominant Alzheimer's Disease Colombia Trial. *Alzheimers Dement*. 2020;16(7):1023-1030.
10. Lopez Lopez C, Tariot PN, Caputo A, et al. The Alzheimer's Prevention Initiative Generation Program: study design of two randomized controlled trials for individuals at risk for clinical onset of Alzheimer's disease. *Alzheimers Dement (N Y)*. 2019;5:216-227.
11. Mills S, Mallmann J, Santacruz A, et al. Preclinical trials in autosomal dominant AD: implementation of the DIAN-TU trial. *Rev Neurol (Paris)*. 2013;169(10):737-743.
12. Sperling RA, Rentz DM, Johnson KA, et al. The A4 study: stopping AD before symptoms begin?. *Sci Transl Med*. 2014;6(228):228fs13.
13. Rabinovici GD, Gatsonis C, Apgar C, et al. Association of amyloid positron emission tomography with subsequent change in clinical management among Medicare beneficiaries with mild cognitive impairment or dementia. *JAMA*. 2019;321(13):1286-1294.
14. Sims JR, Zimmer JA, Evans CD, et al. Donanemab in early symptomatic Alzheimer disease: the TRAILBLAZER-ALZ 2 randomized clinical trial. *JAMA*. 2023;330:512-527.
15. van Dyck CH, Swanson CJ, Aisen P, et al. Lecanemab in early Alzheimer's disease. *N Engl J Med*. 2023;388:9-21.
16. Su Y, Flores S, Wang G, et al. Comparison of Pittsburgh compound B and florbetapir in cross-sectional and longitudinal studies. *Alzheimers Dement (Amst)*. 2019;11:180-190.
17. Navitsky M, Joshi AD, Kennedy I, et al. Standardization of amyloid quantitation with florbetapir standardized uptake value ratios to the Centiloid scale. *Alzheimers Dement*. 2018;14(12):1565-1571.
18. Rowe CC, Doré V, Jones G, et al. (18)F-Florbetaben PET beta-amyloid binding expressed in Centiloids. *Eur J Nucl Med Mol Imaging*. 2017;44(12):2053-2059.
19. Rowe CC, Jones G, Doré V, et al. Standardized expression of 18F-NAV4694 and 11C-PiB beta-amyloid PET results with the Centiloid scale. *J Nucl Med*. 2016;57(8):1233-1237.
20. Klunk WE, Koeppe RA, Price JC, et al. The Centiloid Project: standardizing quantitative amyloid plaque estimation by PET. *Alzheimers Dement*. 2015;11(1):1-15. e1-4.
21. Shah J, Gao F, Li B, et al. Deep residual inception encoder-decoder network for amyloid PET harmonization. *Alzheimers Dement*. 2022;18(12):2448-2457.
22. Chen K, Ghisays V, Luo J, et al, Harmonizing florbetapir and PiB PET measurements of cortical Abeta plaque burden using multiple regions-of-interest and machine learning techniques: an alternative to the Centiloid approach. *Alzheimers Dement*. 2024;20(3):2165-2172.
23. Glodzik L, Rusinek H, Li J, et al, Reduced retention of Pittsburgh compound B in white matter lesions. *Eur J Nucl Med Mol Imaging*. 2015;42(1):97-102.
24. Bodini B, Veronese M, García-Lorenzo D, et al, Dynamic imaging of individual remyelination profiles in multiple sclerosis. *Ann Neurol*. 2016;79(5):726-738.
25. Stankoff B, Freeman L, Aigrot M, et al, Imaging central nervous system myelin by positron emission tomography in multiple sclerosis using [methyl-(1)(1)C]-2-(4'-methylaminophenyl)- 6-hydroxybenzothiazole. *Ann Neurol*. 2011; 69(4):673-680.
26. Bodini B, Veronese M, Turkheimer F, Stankoff B. Benzothiazole and stilbene derivatives as promising positron emission tomography myelin radiotracers for multiple sclerosis. *Ann Neurol*. 2016; 80(1):166-167.
27. Battle MR, Pillay LC., Lowe VJ, et al, Centiloid scaling for quantification of brain amyloid with [(18)F]flutemetamol using multiple processing methods. *EJNMMI Res*, 2018. 8(1):107.
28. Fischl B, FreeSurfer. *Neuroimage*, 2012. 62(2):774-781.
29. Su Y, Blazey TM, Snyder AZ, et al, Partial volume correction in quantitative amyloid imaging. *Neuroimage*, 2015. 107:55-64.
30. Su Y, D'Angelo GM., Vlassenko AG, et al, Quantitative analysis of PiB-PET with FreeSurfer ROIs. *PLoS One*, 2013. 8(11):e73377.
31. Joshi A, R. Koeppe, J. Fessler, Reducing between scanner differences in multi-center PET studies. *Neuroimage*, 2009. 46(1):154-159.
32. Rousset OG, Collins DL, Rahmim A, Wong DF„ Design and implementation of an automated partial volume correction in PET: application to dopamine receptor quantification in the normal human striatum. *J Nucl Med*, 2008. 49(7):1097-1106.
33. Lucy L, An iterative technique for the rectification of observed distributions. *Astronom J*. 1974. 79:745.
34. Biggs D, M. Andrews, Acceleration of iterative image restoration algorithms. *Appl Optics*, 1997. 36(8):1766-1775.
35. Steiger J, Tests for comparing elements of a correlation matrix. *Psychol Bull*, 1980. 87(2):245-251.
36. Su Y, Blazey TM, Owen CJ, et al, Quantitative amyloid imaging in autosomal dominant Alzheimer's disease: results from the DIAN Study Group. *PLoS One*, 2016. 11(3):e0152082.

SUPPORTING INFORMATION

Additional supporting information can be found online in the Supporting Information section at the end of this article.

How to cite this article: Chen Y, Protas H, Luo J, et al. Accounting for white matter uptake improves between tracer agreement in amyloid PET. *Alzheimer's Dement*. 2025;17:e70165. https://doi.org/10.1002/dad2.70165